Available online at www.sciencedirect.com
SCIENCE DIRECT®
Materials and Design 25 (2004) 145–154
Materials & Design
www.elsevier.com/locate/matdes

Low temperature polymer infiltration for rapid tooling

Jack G. Zhou [a,*], Monnappa Kokkengada [a], Zongyan He [a], Yun S. Kim [a], Ampere A. Tseng [b]

[a] Department of Mechanical Engineering and Mechanics, Drexel University, Philadelphia, PA 19104, USA
[b] Manufacturing Institute, Arizona State University, Tempe, AZ 85287-5106, USA

Abstract

Common infiltration methods used in rapid tooling have certain limitations viz., cracks, distortion and shrinkage caused by high temperature infiltration. Poor surface quality is also a limitation of conventional infiltration techniques. The high temperatures involved in conventional infiltration techniques make the process more expensive, complex and difficult to control. To overcome these difficulties, as well as to generate tooling for a small batch production, a low temperature polymer infiltration method has been developed in conjunction with existing rapid tooling techniques. Based on the curing principles of polymer materials, several infiltration materials were selected and their mechanical and chemical characteristics were investigated. To determine the necessary amount of polymer materials and infiltration height in the sintered mold an infiltration model is derived and results compared with experimental data. Testing results have shown significant improvements in the thermal resistance and mechanical properties of the rapid tool as a result of the resin infiltration.

Keywords: Polymer infiltration; Rapid tooling; Mechanical testing

1. Introduction

Often in a product development lifecycle, prototypes made from the final product material are required to generate accurate results; in order to achieve this it is desirable to generate tooling capable of producing a small number of production parts hundreds or few thousands. The research presented in this paper is an effort toward developing such a technique. Rapid prototyping/tooling and manufacturing have experienced tremendous growth and have drawn great attention in national and international manufacturing industry [1]. Although rapid prototyping has brought in a new revolution in manufacturing processes by using additive layer by layer material processing technique, its focus has gradually shifted to rapid tooling/manufacturing, i.e., not only prototypes but also functional products. The development list of Rapid Tooling (RT) technology based on rapid prototyping and manufacturing has been growing in recent years [2]. Several RT techniques have been proposed, and examples are 3D Systems' Keltool process, DTMs RapidSteel, Extrudehone's PROMETAL [3] and Rapid Pattern Based Powder Sintering (RPBPS) technique [4,5]. Most RT techniques involve sintering a cast powder compact and then infiltrating the sintered compact with a low melting temperature metal like copper or alloys like brass, bronze, etc. The composition of the sintered compact is approximately 30–40% porosity and 70–60% metal. In MIT's 3D printing the sintered compact is 63% metal and 37% porosity [6] and in Drexel's RPBPS technique the sintered compact is 64% metal and 36% porosity [4,5], while DTM's RapidSteel process produces a sintered compact 60% metal and 40% porosity [7]. This research aims to develop a low temperature infiltration stage for rapid tooling. The low temperature infiltration stage is designed to overcome the problems of large shrinkage, distortion and cracks that are associated with traditional high temperature metal infiltration techniques. Additionally, this low temperature infiltration technique can be used in any of the existing RT processes for producing short run production parts. This would greatly enhance

* Corresponding author. Tel.: +1-215-895-1480; fax: +1-215-895-1478.
E-mail address: zhoug@drexel.edu (J.G. Zhou).

0261-3069/$ - see front matter © 2003 Elsevier Ltd. All rights reserved.
doi:10.1016/j.matdes.2003.09.014

the capabilities of these techniques and make them more attractive to a wider spectrum of users. The additional step will be more economical and faster than the existing high temperature infiltration techniques that these RT processes presently use. The paper is structured as follows. First, there is a study on infiltrants. Three low temperature infiltration methods are introduced. A model of the infiltration process is deduced and compared with experimental data. Further, the microstructure, thermal and mechanical properties of the infiltrated samples are tested and finally results are evaluated.

2. Material study on infiltrants

2.1. Requirements of potential infiltrants

An ideal infiltrant should completely fill the pore space, and exhibit good flow and wetting of the pore structure. Based on the experience with RPBPS several requirements for any suitable infiltrant were identified:

- It should be liquid at room temperature but should transform to a solid under suitable conditions.
- The liquid to solid transformation should be irreversible.
- The change in volume during the liquid to solid transformation should be as small as possible.
- The infiltrant should have a low viscosity and a high wettability for the metal powder so as to enable the infiltrant to soak into the sintered compact and fill the pores.
- On solidification, the infiltrant should possess reasonable strength, hardness and chemical resistance so as to be used for injection molding.
- The infiltrant material should be able to resist temperatures of 150–200 °C, which is what an injection mold needs to withstand when processing common polymers like ABS, PVC, polycarbonate and PE.

2.2. Selection of potential infiltrants

A quick overview of the above conditions automatically eliminated metals and ceramic materials, as they do not satisfy most of the above conditions. Organic materials, i.e., polymers usually have low strength and hardness and they cannot withstand higher temperatures, however certain polymers, especially thermosetting resins, do meet the above-mentioned requirements and merit further investigation. After a survey of available resins that satisfy above criteria several potential infiltrants were selected.

2.3. Properties of selected infiltrants

2.3.1. Phenolic resin

Phenolic resin is classified as a condensation reaction polymer. In this type of reaction, the polymer grows by combining two large molecules and releasing a third small molecule, usually water. A wide range of characteristics can be designed into a phenolic resin such as reactivity, moisture, molecular weight, pH value, monomer level, viscosity, flow rate and lubrication. A key property of phenolic resin is the ability to withstand higher temperature. Unlike most polymers, the glass transition temperature (Tg) of phenolic resin can be further elevated to 260 °C by suitable design. Considering that an injection mold needs to bear a temperature of 100 °C to 200 °C to manufacture common plastic parts, phenolic resin can be selected for the infiltration of an injection mold. The phenolic solution can penetrate and soak into the sintered compacts easily for most of metal powder materials, its curing temperature is around 150 °C, and its shrinkage during the curing process depends mainly on the density of the solution. For the phenolic solution the lower the viscosity, the lower the density, and the larger the shrinkage will be. Main specifications of the resin used (Plenco 06582) are listed in the last column of Table 1.

2.3.2. Epoxy resin

Most epoxy resins have high viscosity and low thermal-resistance. However, some modified epoxy resins can be used as ideal infiltration candidates. For example, the viscosity of resin AboCast 50-3 is 110 cP (at 70 °C), similar to light motor oil, and the viscosity of AboCast 50-6 and AboCast 50-24 is much less than 110 cP (see Table 1). However, as mentioned above, the resin with lower viscosity will have a lower density/strength and thermal-resistance and a larger shrinkage. Users should compare all properties of various resins to make their selections. Table 1 shows main properties of the selected resins and it can be seen that their viscosity, strength, thermal property and chemical resistance are all suitable for injection-mold applications.

2.3.3. Acrylic resin

The IMPREX SUPER SEAL 95-1000A manufactured by Imprex Inc., is a thermosetting resin composed of mixed methacrylate monomers and unsaturated polyester. This resin is pre-catalyzed with azodiisobutyronitrile and water and it has a specific gravity of 1.064 and a boiling point of 163 °C. The resin is a pale straw colored liquid with a slight blue tinge and a pleasant odor. This resin is free from any hazardous components and is not carcinogenic. From the experiments, it has been observed that the viscosity of the resin is relatively stable with increase in temperature and is 16 cP at 25 °C. In the heating process, the resin is stable until around 80 °C and any heating above this temperature will result in the resin crosslinking to form a white translucent solid. The viscosity of the resin at various temperatures, between room temperature and curing

Table 1
Typical properties of infiltration materials

Resin	AboCast 50-3	AboCast 50-6	AboCast 50-24	Plenco 06582
Hardener	Cure50-17	Cure50-17	Cure50-17	
Ratio (resin/hardener) by wt.	100/26	100/28	100/115	100/0
BI. viscosity (cP/°C)	110/70	70/70	80/25	50/25 (50% alcohol)
Specific gravity ($H_2O = 1$)	1.87	1.75	1.89	1.59
Flexural strength (MPa)	94.9	107.3	90.5	93.8
Flexural modulus (MPa)	3,900	3,520	3,450	7,952
Tensile strength (MPa)	67.1	70.3	57.8	59.0
Tensile modulus (MPa)	3,750	2,170	4,250	8,982.0
Compressive strength (MPa)	118.1	124.0	110.6	115.0
Tensile elongation (%)	4.4	3.0	4.7	0.7
Hardness, Rockwell	106(M scale)	109(M scale)	104(M scale)	42(E scale)
Mold shrinkage (m/m)	0.001	0.0012	0.002	0.0023
Deflection temperature (°C)	160	157	170	221
Heat resistance (°C)	230	257	298	238
Thermal degradation (wt. loss) After 100 h, 160 °C	0.55%	0.44%	0.65%	N/A
Chemical resistance (wt. loss) After 120 days, 30% sulfuric acid	2.60%	1.96%	1.96%	N/A
Cure temperature and time (°C/h)	80/1.5	80/2.5	25/14	80/(12–20)

temperature has been determined and the plot of viscosity versus temperature is shown in Fig. 1.

It can be seen from the figure that the acrylic resin has a very low viscosity that decreases with temperature increase. The low viscosity and stability at room temperatures are the most attractive properties of the resin that urged us to investigate its usefulness as an infiltrant for this technique. Additionally the polyester component provides enhanced chemical and thermal resistance [8].

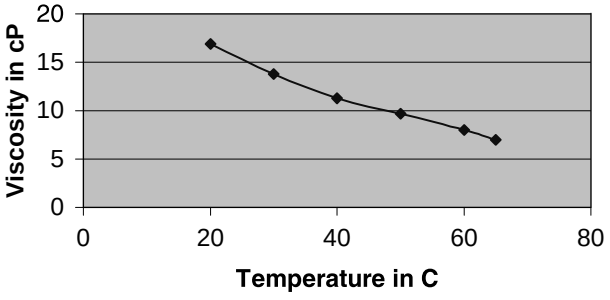

Fig. 1. Variation of viscosity with temperature for the acrylic resin.

3. Three infiltration methods

Usually the green compact is sintered before infiltration and the surface of the compact is cleaned to remove any surface oxidation that may have been formed during the sintering. Some resins have a high viscosity at room temperature and they cure with time, i.e., their viscosity increases with time even at room temperature. A gradual infiltration process of a mold with large wall thickness would result in the infiltrant curing at the outer walls leaving the central core of the mold porous. To overcome this problem three methods of infiltrating the sintered compact based on the viscosity of the infiltrant and their curing properties have been devised (Fig. 2).

Method (A) is employed when the mold wall thickness is large and the curing occurs at room temperature. In this method, the inner surface of the mold does not

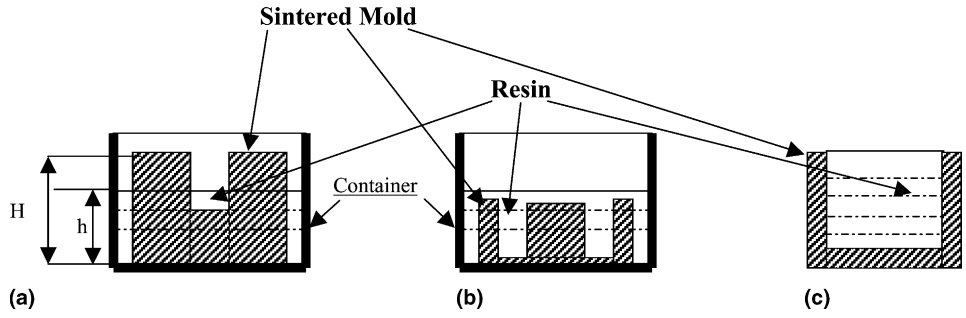

Fig. 2. Three methods of infiltrating sintered mold.

come into contact with the resin and the resin infiltrates from bottom upwards. In order to ensure complete infiltration of the mold before curing occurs the whole container is placed into a refrigerator let the entire mold be infiltrated. The mold is then exposed to an ambient or warmed temperature to enable it to be cured.

Method (B) is used when the infiltrant has a low viscosity and remains a constant at ambient temperature. In this method, the entire mold is submerged into the resin let all the pores be filled with the infiltrant. The infiltrated mold is then removed and heated to the curing temperature of the infiltrant until the resin cures.

Method (C) is employed when the mold has thin walls and the inner surface of the mold is free from any surface designs that might be damaged from contact with the resin. In this method the resin is poured directly into the mold cavity to allow it to infiltrate the sintered compact from top downwards. More resin can be added in as required until the whole mold is infiltrated and the mold is then heated to cure the resin.

For the infiltration to be successful all the pores of the green compact should be filled, the mold surface should be clean and free from any imperfections to facilitate the infiltration process. In order to achieve complete filling, a model of the infiltration process to calculate the amount of infiltrant needed to infiltrate a given mold has been developed.

4. Modeling the infiltration process

For a liquid the capillary pressure δP varies inversely with the pore size d [9,10] as shown in,

$$\delta P = 2\gamma \cos\theta / d, \tag{1}$$

where γ denotes surface energy of the liquid, θ denotes contact angle and d denotes radius of the pore.

It can be seen from the equation that the capillary effect depends on three factors: surface tension of the resin, size of the pore and the angle between the sintered powder and resin which is representative of the wettability of the resin to the powder. From the above Eq. (1), it can be seen that greater capillarity is achieved when the pore sizes are smaller and the contact angle is smaller. The height that the liquid (resin) raises due to the capillary pressure is given by

$$\delta H = \delta P / \rho, \tag{2}$$

where ρ is the weight density of the resin.

The above equations cannot be used directly to calculate the infiltration height of a sintered mold because the voids in the sintered mold are not straight circular tubes as assumed in the derivation of the above equation. An equivalent radius r', i.e., the radius of a circular cross-section that has the same area as that of the void in the sintered mold should be derived. The equivalent radius r' is related to the size of the powder particles and the gap ratio (λ). As shown in Fig. 3 it is assumed that the microstructure of the sintered mold can be simplified to be a collection of straight circular cylinders that are bonded together during sintering. The packing arrangement of these cylinders can be any one of those shown in Fig. 4. Each mode has its own gap ratio based on the structure of packing.

For mode (a), it has $\lambda_a = [S_{abc} - 3(\pi R^2)/6]/S_{abc} \approx 0.092$, where R is the radius of the particle and S_{abc} is the area of equilateral triangle abc. For mode (b), it has $\lambda_b = [S_{abcd} - 4(\pi R^2/4)]/S_{abcd} \approx 0.215$ where S_{abcd} is area of square abcd. For mode (c), it has $\lambda_c = [S_{abcdef} - 4(\pi R^2/4)]/S_{abcdef} \approx 0.395$, where S_{abcdef} is area of hexagon abcdef.

The experiments have shown that the gap ratio in sintered parts is between 0.30 and 0.40, so mode (b) with gap-ratio 0.215 and mode (c) with gap-ratio 0.395 would be appropriate models for our infiltration process.

Now the equivalent radius r' for mode (b) can be deduced. The area occupied by the infiltrated resin = Area of square abcd − 4 * (Area of quadrant), i.e., $S_r = (2R)^2 - 4(\pi R^2/4)] = \pi r'^2$, where S_r is the equivalent circular cross-section, so it has

$$r' = (\sqrt{4/\pi - 1})R. \tag{3}$$

It has been know that $\lambda_b = S_r/(2R)^2$ therefore

$$r' = [\sqrt{4\lambda_b/\pi}]R. \tag{4}$$

The equivalent radius for mode (c) can also be derived. The area occupied by the infiltrated resin = Area of

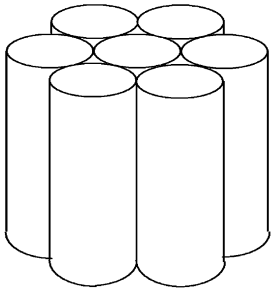

Fig. 3. Assumption of the microstructure of sintered mold.

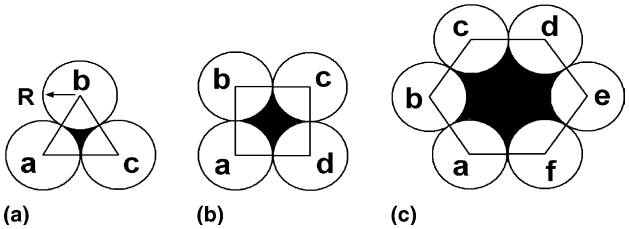

Fig. 4. Packing modes of sintered powder particles.

hexagon abcdef $-6*$(Area of sector), i.e., $S_r = [6\sqrt{3}(R^2) - 2\pi R^2] = \pi r'^2$, where S_r is the equivalent circular cross-section, so it has,

$$r' = \sqrt{(6\sqrt{3}/\pi) - 2}R. \tag{5}$$

It has been known that $\lambda_c = S_r/(6\sqrt{3}R^2)$ therefore

$$r' = \sqrt{6\sqrt{3}\lambda_c/\pi R}. \tag{6}$$

Let the d in Eq. (1) be replaced by the r' derived in Eqs. (4) and (6). Substituting the result in Eq. (2) for infiltration height, the following relationships can be deduced

$$\delta H = \sqrt{\pi}\sigma\cos\theta/(\rho R\sqrt{\lambda}) \approx 1.77\sigma\cos\theta/(\rho R\sqrt{\lambda}) \quad \text{for mode (b)} \tag{7}$$

and

$$\delta H = 2\sqrt{\pi}\sigma\cos\theta/\left(\sqrt{6\sqrt{3}}\rho R\sqrt{\lambda}\right). \approx 1.10\sigma\cos\theta/(\rho R\sqrt{\lambda}) \quad \text{for mode (c).} \tag{8}$$

For water as the infiltrant: $\rho = 1$ g/cm^3, $R = 50 \times 10^{-6}$ m, $\lambda = 0.3$, $\sigma = 7.3 \times 10^{-2}$ N/m. From the above equation, the height that water can infiltrate due to capillary pressure is 2.932 m. For brass as the infiltrant: $\rho = 6.4$ g/cm^3, $R = 50 \times 10^{-6}$ m, $\lambda = 0.3$, $\theta = 0°$, $\sigma = 0.12$ N/m. From the above equation, the height that brass can infiltrate due to capillary pressure is 0.75 m. For acrylic resin as the infiltrant: $\rho = 1.064$ g/cm^3, $R = 50 \times 10^{-6}$ m, $\lambda = 0.3$, $\theta = 150$, $\sigma = 5.5 \times 10^{-2}$ N/m. From the above equation, the height that the acrylic resin can infiltrate due to capillary pressure is 2.004 m.

The above calculations show that depending on the thickness of the mold and the nature of the infiltrant the appropriate mode of infiltration should be chosen. The real infiltration height will be less than the calculated value because the real microstructure of the sintered mold is not composed of uniform tubes and the contact angle is not so small due to the rough surface state of the powder particles.

An important factor to be considered during infiltration with a resin is the curing time of the resin. The epoxy resin is a two-part resin that cures at room temperature. This results in that the resin curing before it can infiltrate a part of desired height. Thus the maximum height that a resin can infiltrate is limited by the property of the resin. The acrylic resin on the other hand does not suffer from this drawback, in that it is cured only on heating to its curing temperature of 80 °C.

5. Prediction of infiltration rate

The infiltration rate depends on the amount of porosity. Experiments were conducted on samples made by our RPBPS technique to estimate the time required to infiltrate the sintered compact using the acrylic resin. The volume ratio of the porosity in the sintered compact was found to be 36%.

Infiltration takes place due to the rise of resin into the pores by capillary action. The larger the surface area of the compact exposed to resin the faster is the rate of infiltration due to the fact that a larger number of pores are exposed to the resin. It is attempted to develop a model to predict the time for infiltration for any given compact. As seen in Fig. 5, let L be the length of the sintered compact, B the breadth of the compact, and H the height of the compact. Let h be the height submerged by the resin. The volume of the compact (V_s) and the volume of porosity in compact (V_p) can be calculated as follows:

$$V_s = LBH, \tag{9}$$

$$V_p = 0.36[LBH]. \tag{10}$$

An estimate of the time to infiltrate any given sample can be defined as:

Time for total infiltration
= Volume of porosity/rate of infiltration,

$$T = V_p/X, \tag{11}$$

where X is the rate of infiltration of the resin into the sintered compact. The experiments have shown that the value of X is 1.35 cm^3/min. The above expression helped to determine fairly accurately the time to infiltrate a given sample (Table 2). The time to infiltrate the sample depends not only on the volume of porosity but also on the area of the compact exposed to the resin. This area is

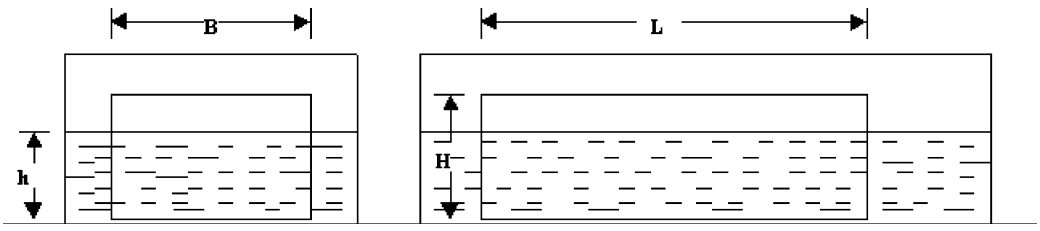

Fig. 5. Model to calculate time of infiltration of sintered compact.

Table 2
Variation of infiltration time with infiltration area

Volume of sample, V_s (cm^3)	Volume of porosity, V_p (cm^3)	Infiltration area, A_I (cm^2)	A_I/V_s	Actual infiltration time (min)	Theoretical infiltration time (min)	Rate of infiltration (cm^3/min)
92.69	33.37	24.63	0.266	20.2	24.6	1.66
32.77	6.92	13.935	0.425	10.1	8.73	1.38
19.22	11.8	8.1	0.421	5.1	5.125	1.18
9.79	3.52	4.875	0.498	3.0	2.61	1.17

called the Effective Infiltration Area. From Fig. 5 it can be seen that:

Surface area of compact exposed to resin

$$= 2[Bh + Lh] + [BL]. \quad (12)$$

It is assumed that 36% of this surface area is actually composed of porosity. Thus,

Effective Infiltration Area(A_I)

$$= 0.72[Bh + Lh] + 0.36[BL]. \quad (13)$$

The ratio of effective infiltration area with the volume of the sintered compact (A_I/V_s) can be seen in Table 2.

It can be seen that as the A_I/V_s ratio increases the time for infiltration decreases implying that as the effective area for infiltration increases with respect to the volume of sample, the time required to infiltrate the sample decreases. The average rate of infiltration of 1.35 cm^3/min gives a fairly accurate prediction of the time needed to infiltrate a sintered compact if its volume is known. This value of rate of infiltration was determined for the Imprex resin for room temperature infiltration. This value depends on the properties of the resin such as curing time and curing temperature. From the above table, it also can be seen that the actual infiltration times are very close to the theoretical infiltration times. The above model helps to determine the time needed to infiltrate a sample given its volume and the volume ratio of its porosity.

6. Microstructure analysis

Samples of tool steel were cast and sintered using the RPBPS technique. These samples were then infiltrated using the phenolic resin, epoxy resin and the acrylic resin using method A shown in Fig. 2. Fig. 6 shows typical microstructures of the infiltrated samples. These Scanning Electronic Microscope (SEM) photos came from different positions in the samples. Photo (a) shows microstructure in a completely infiltrated region, from which it can be seen that almost all gaps and holes have been filled with the resin, and between the resin and particles there is a good bonding layer, i.e., on the boundary there are no obvious defects. Photo (b) came from a transition region; the upper part has been infiltrated and the lower part has not been infiltrated yet, and the gaps and holes have black color. Photo (c) came from a special region, in which some carbon particles (came from binder thermal decomposition) still remain on the surface of the metal particles so that the resin cannot directly contact with metal particles. Since the

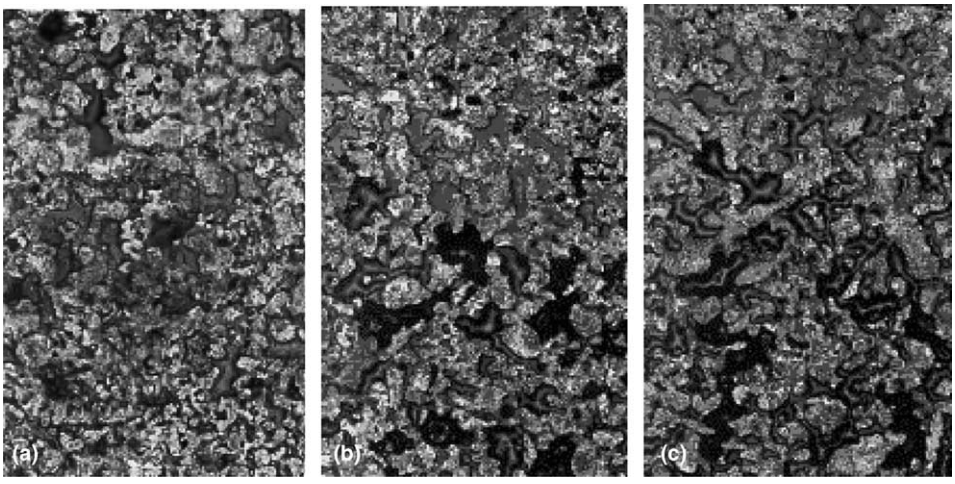

Fig. 6. SEM photos on the microstructures of infiltrated specimens.

wettability of the resin to the carbon is poor, the resulted bounding condition is not good. From the photo it can be seen that the resin cannot fill in the entire material, and black gaps between resin and metal particles appeared. Because of the poor infiltration, the mechanical properties and chemical resistance of the product will be reduced. It is strongly recommended that the green compact must be sintered carefully and completely to remove all carbon deposits.

Injection molding is a process in which a polymer is heated to a highly plastic state and forced to flow under high pressure into a mold cavity, where it solidifies. The molded part, called a molding, is then removed from the cavity. Injection molding is also used for thermosetting (TS) plastics, with certain modifications in equipment and operating procedure to allow for crosslinking. The modified injection-molding machines utilize a reciprocating-screw injection unit, but the barrel length is shorter to avoid premature curing and solidification of the TS polymer. For the same reason, temperature in the barrel is kept at relatively low levels, usually 100–260 °C, depending on the polymer. The molding cycle time typically ranges from 20 s to 2 min, depending on polymer type and part size. A polymer infiltrated mold has been tested based on a simulation of the injection-molding process. This test is set with a temperature range from 24 to 100 °C and a 1-min cycle as shown in Fig. 7.

The experimental steps are: (a) to set the oven to temperature 100 °C, (b) to put the sample in the oven for heating for 1 min, (c) to put the sample in cold water set for cooling for 1 min, (d) to observe the sample surface, (e) to repeat steps (b)–(d) for 50–100 times. This experiment has been made to test the selected infiltration materials. The results show that epoxy resin, phenolic resin and acrylic resin have enough thermal resistance when the temperature is below 150 °C. But when the temperature is over 150 °C the epoxy resin will lose some weight through decomposition, and the surface of the sample infiltrated with epoxy resin will become dirty and sticky. Phenolic resin shows a much higher thermal resistance, even when the temperature reaches 250 °C, the surface of the sample is still very smooth and without any changes.

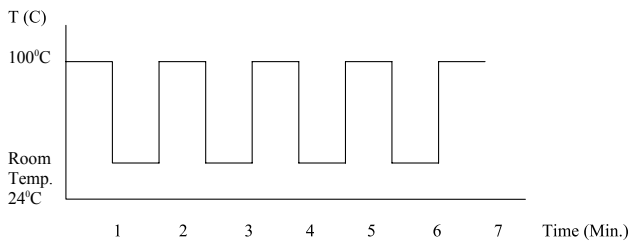

Fig. 7. The program for simulating the injection-molding machine process.

7. Mechanical testing

The mechanical properties of powder metallurgy parts are degraded by the presence of pores. Strength is the first concern when dealing with most structural powder metallurgy components. At a given porosity, smooth pores give better strength. The dynamic properties of powder metallurgy parts are sensitive to the subtle microstructural details. The pores act as fatigue crack initiation sites and contribute to low fracture toughness. Thus in evaluating a powder metal part it is logical to first inspect strength.

Several standard tests for mechanical properties can be applied to powder metallurgy materials. A radial crush strength test is the basis for analyzing the properties of sintered products such as cylindrical bearings. The transverse rupture strength is the most common measure of the strength of low ductility powder metallurgy parts. Bend tests establish the ductility of a metal under bending stress and show the ability of the metal to withstand breakdown in use; additionally the bend test provides a reasonable guide to tensile strength too [11]. The transverse rupture strength test is performed on a rectangular specimen in a three point bending set up to test the change in mechanical properties as a result of the low temperature infiltration. The bending tests for samples infiltrated with the epoxy resin and acrylic resin have been conducted to show the general improvement in the mechanical properties as a result of the low temperature resin infiltration.

Several steel powder green compacts in the shape of 1-in. square bar (dimension: 1 in. × 1 in. × 5 in.) were sintered in a furnace up to 760 °C. After sintering, one group named sintered-only was tested for strength and hardness. The other group named sintered + infiltrated was infiltrated with the resin and then also tested for strength and hardness. Figs. 8(a) and (b) show the results of the bending test of the two groups for the epoxy resin infiltration. Figs. 9(a) and (b) show the results of the bending test for the acrylic resin infiltration. In the case of the epoxy resin it can be seen that the sintered-only sample (see Fig. 8(a)) has a maximum stress 33.2 MPa, while the sintered + infiltrated sample (see Fig. 8(b)) has a maximum stress 47.7 MPa showing a 43.7% increase. It also can be seen that Fig. 8(b) has a better stress–strain ratio than that of Fig. 8a. The hardness of the sintered-only is 1 HRA, and the sintered + infiltrated sample is 20 HRA, which gives a 20 times increase. The shrinkage of the sintered + infiltrated part is 0.4%, which has a 6.25–7.5 times reduction comparing to the brass infiltrated part which usually has 2.5–3.0% shrinkage. There is no cracks and visible distortions from the sintered + infiltrated part.

In the case of the acrylic resin, it can be seen that the maximum bending stress before infiltration (see Fig. 9(a)) is 59.3 MPa and the maximum bending stress

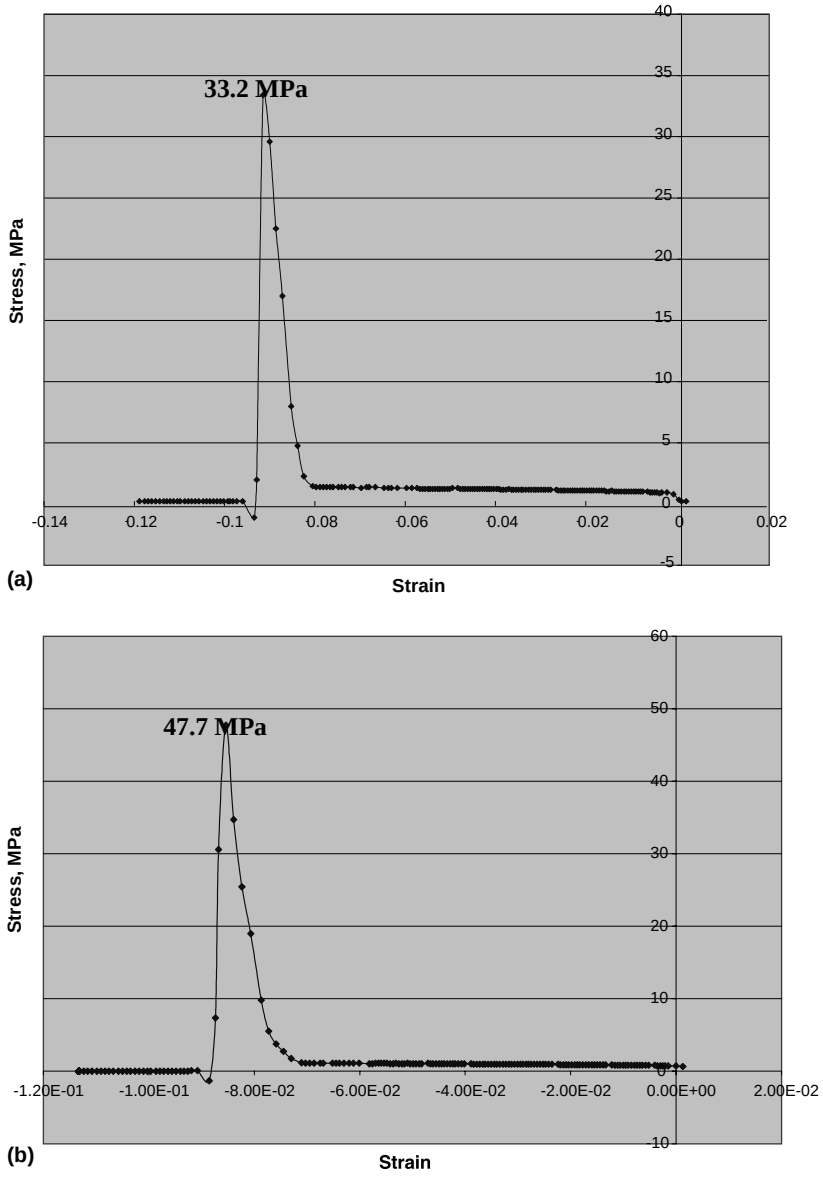

Fig. 8. (a) Stress–strain plot from bending testing for the sintered-only sample. (b) Stress–strain plot from bending testing for the sintered + epoxy resin infiltrated sample.

after infiltration (see Fig. 9(b)) is 82.8 MPa. There is a 39.8% increase in the bending stress as a result of the infiltration. The sample was weighed before and after infiltration and an 8.2% increase in the weight of the sample was found as a result of the infiltration. The sintered sample was too soft to give a reading on the regular Rockwell scales so the superficial Rockwell test was conducted on the sintered sample as well as the infiltrated sample. The hardness was tested by using a 15 kg major load and a 1/16″ ball in T scale. It has been received that readings of Rockwell 15 T, 35.3 for the sintered part and Rockwell 15 T, 41.3 for the sintered and infiltrated part. This is similar to some varieties of steel tinplate. The above data shows that there is a 17.2% increase in the hardness of the part due to infiltration. The acrylic resin gave a shrinkage of less than 0.5% that is considerably lower than that of conventional infiltration techniques with brass or bronze or copper.

The samples prepared with different binder resins showed a wide variation in their mechanical properties due to the difference in the properties of the two binders. Yet these results show that the low temperature polymer infiltration method whether using epoxy resin or acrylic resin could increase the product strength (yield stress and maximum bending stress) and hardness significantly, and reduce the shrinkage and distortion to the minimum.

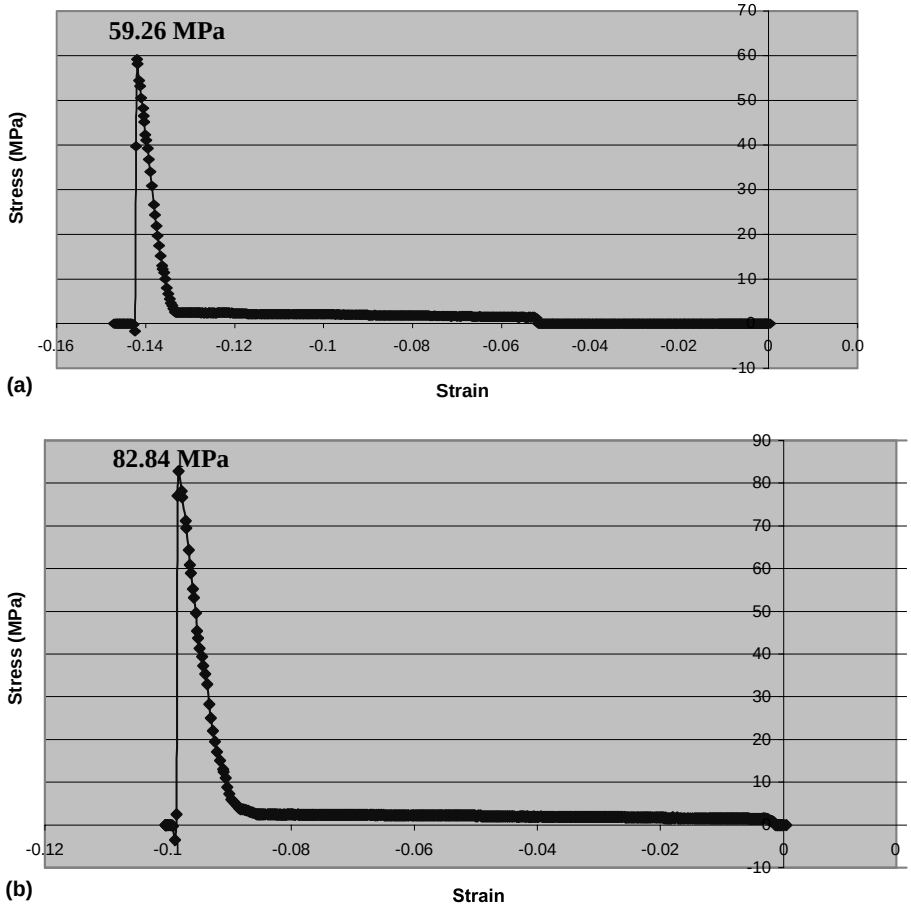

Fig. 9. (a) Stress–strain relationship of sintered sample. (b) Stress–strain relationship of sintered + acrylic resin infiltrated sample.

8. Discussion and conclusion

This research is still in its initial stage. There are several questions existing for further study. Comparing with conventional metal (e.g., copper, brass/bronze) infiltration, the strength and hardness of the polymer-infiltrated product is much lower and it cannot bear high temperature (more than 200 °C). A new group of resins should be developed to have high solidification strength and hardness, high decomposition temperature, and low viscosity. Curing conditions for each resin are different, some times they are very hard to follow and control. A convenient and regulated curing process for the polymer infiltration process should be developed.

By developing a low temperature infiltration stage a technique that can be used by existing RT techniques to generate soft tooling capability for short run production parts both economically and rapidly has been developed. The research has deduced an infiltration model to analyze the low temperature infiltration so as to be able to estimate the time of infiltration and the infiltration height in the sintered compact, and has verified the model with experimental data. The new technique overcomes the defects of conventional high temperature infiltration like cracks and also serves to reduce shrinkage and distortion appreciably. The new infiltrants serve to improve the yield stress and hardness of the sintered part. These infiltrants though do not improve the mechanical properties as much as traditional infiltrant materials like copper yet this method is useful in that it helps to extend the range of existing RT techniques to include a new segment of the tooling market while simultaneously overcoming the drawbacks of existing high temperature infiltration techniques. The unique feature of the technique is that it can be combined with any existing RT technique without any major changes in their existing process and whatever be the material of the tooling this infiltration technique can be utilized.

References

[1] Jacobs PF. Stereolithography and other RP&M technologies from rapid prototyping to rapid tooling. NewYork: SME Press; 1996.

[2] Vanputte DA. Rapid Tooling is a Key Factor in Future Achieving Rapid Product Development, Proceeding of 27th ISATA Conference, Auchen, Germany, Paper No. 94RA024 1994.

[3] Ashley S. Rapid prototyping industry's growing pains, Mech Eng, ASME July 1998;64–8.
[4] Zhou J, He Z. Rapid pattern based powder sintering technique and related shrinkage control. J Mater Des 1998;19:241–8.
[5] Zhou J, He Z. A new rapid tooling technique and its special binder study. J Rapid Prototyping 1999;5(2).
[6] Sachs E, Allen S, Cima M, et al. Fabricating Metal Tooling and Metal Parts by 3D Printing, Solid Freeform Fabrication Symposium Proceedings, The University of Texas at Austin, 1998.
[7] Nelson C. RapidSteel 2.0 Mold Inserts for Plastic Injection Molding. Available http://www.dtm-corp.com, 1998.
[8] Muisener CM. Resin impregnation of powder metal parts. Powder Metal Technol Appl ASM Handbook 1998;7.
[9] German RM. Powder metallurgy science. second ed. New Jersey: Metal Powder Industries Federation; 1997.
[10] Sears FW, Zemansky MW, Young HD. University physics. sixth ed. Massachusetts: Addison-Wesley; 1984. reprinted in Feb.,1984, pp. 253–5.
[11] Simons EN. Testing of metals. Great Albion Books; 1972.